研究成果の刊行に関する一覧表
(2006年4月1日ー2007年3月31日迄)

名前〈小泉　修一〉

書籍

小泉修一（2006）グリア細胞によるシナプス伝達制御に関する研究.　ブレインサイエンス・レビュー2006（伊藤正男、川合述史　編）、105-120.

雑誌

発表者氏名	論文タイトル名	発表誌名	巻号	ページ	出版年
Koizumi, S., Shigemoto-Mogami, Y., Nasu-Tada, K., Shinozaki, Y., Ohsawa, K., Tsuda, M., Joshi, B.V., Jacobson, K. A., Kohsaka, S. and Inoue, K	UDP acting at $P2Y_6$ receptors is a novel mediator of microglial phagocytosis.	Nature			in press
Shinozaki, T., Koizumi, S., Ohno, T., Nagao, T. and Inoue, K.	Extracellular ATP countrtacts the ERK1/2-Mediated Death-Promoting Signaling Cascades in Astrosytes	Glia	54	606-618	2006
Tozaki-Saito, H., Koizumi, S., Sato, Y., Tsuda, M., Nagao, T. and Inoue, K.	Retinoic acids increase $P2X_2$ receptor expression through the 5'-flanking region of P2rx2 gene in rat phaeochromocytoma PC12 cells.	Mol. Pharmacol.	319-328	319-328	in press
小泉修一、藤下加代子、津田誠、井上和秀	ATP を介した皮膚ケラチノサイト間情報連絡と痛み	**Pain Research**	21,	133-139	2006
小泉修一、藤下加代子、津田誠、井上和秀	G 蛋白質共役型 ATP 受容体と痛み	ペインクリニック	27	560-568	2006

厚生労働科学研究費補助金（医薬品医療機器等レギュラトリーサイエンス総合研究事業）
平成18年度　分担研究報告書
「血液脳関門破綻に基づく医薬品副作用の予測系の確立」に関する研究

In vitro BBB病態モデル作成及び各種薬物の脳内移行性評価

分担研究者：片岡　泰文　福岡大学薬学部・教授

研究要旨
薬物の脳移行は血液脳関門（BBB）により制限されている。薬物の中枢性副作用発現機序を明らかにするためには、BBB透過性を評価する必要がある。また、ある種の病態下ではBBB機能が変容することが知られている。従って、in vitroで病態時のBBBを再現しうるモデルの開発は、薬物の中枢性副作用の発現機序解明、予測・回避対策構築に有用である。本研究では、BBB構成細胞である脳血管内皮細胞、アストロサイトおよびペリサイトから成る新規in vitro BBBモデルおよび発熱・炎症病態時のBBBモデルの作製を試みた。ラット脳よりBBB構成細胞を単離後、7種類の単層培養あるいは共培養BBBモデルを作成し、BBB機能を比較検討した。7種類のモデル中、3種の構成細胞からなる共培養モデルが最もBBB機能が亢進していた。このBBBモデルは解剖学的にも生体に類似したものであり、3種細胞間のクロストークはBBB機能の維持に必要であると考えられる。また、高温負荷培養条件下あるいはLPS刺激によりBBB機能は低下した。これらのモデルは常態時および発熱・炎症病態時の薬物脳移行性を簡便に評価する検定キットとして有用である。

A．研究目的

薬物の脳移行は血液脳関門（BBB）により制限されている。薬物の中枢性副作用発現機序を明らかにするためには、薬物の脳移行性すなわちBBB透過性を評価する必要がある。また、ある種の病態化ではBBB機能が変容することが知られている。従って、in vitroで病態時のBBBを再現しうるモデルの開発は、薬物の中枢性副作用の発現機序解明、予測・回避対策構築に有用である。BBBは脳血管内皮細胞、アストロサイトおよびペリサイトから構成され、これら細胞間のクロストークがBBB機能の発現や維持を制御することが明らかになりつつある。そこで、本研究では、新規in vitro BBBモデルの確立を目指して、3種のBBB構成細胞を用いた各種BBBモデルを作成し、その密着結合性および輸送タンパク質発現量を比較した。

また、NSAIDsによるインフルエンザ脳症の発現機序とBBB透過性との関連を明らかにするために、発熱・炎症病態時BBBモデルの構築を目指して、熱負荷BBBモデルおよびLPS刺激BBBモデルの機能評価を行った。

B．研究方法

1）新規in vitro BBBモデルの開発

①BBBモデルの作成：

ラットより脳毛細血管内皮細胞、ペリサイトおよびアストロサイトを既報に従い単離した。モデルの作成は、Transwell®システムを用い、脳血管内皮細胞をメンブラン上に播種し、内皮細胞のみの単層培養系および任意の細胞2種あるいは3種からなる共培養系BBBモデルを

びEBA透過性を亢進させた。発熱はBBB機能低下の危険因子になり得ると推察される。また、同様にミクログリア共培養 BBB モデルにおいて、LPS 刺激は透過性亢進作用を示した。LPS 刺激により産生される炎症性サイトカイン類はBBB機能を低下させることが知られている。これらのモデルは、インフルエンザ等の発熱・炎症性疾患時の BBB モデルとして薬物の病態依存的な脳移行性の評価に使用できる。

E．結論

本研究では、簡便なBBB透過性評価を可能とする新規 in vitro BBB モデルおよび発熱・炎症病態BBBモデルを確立した。本モデルは常態時あるいは病態時の薬物の脳移行性を評価するうえで有用なツールとなり得る。

F．健康危機情報

なし

G．研究発表

1．論文発表

Takata F, Dohgu S, Yamauchi A, Sumi N, Nakagawa S, Naito M, Tsuruo T, Shuto H, Kataoka Y: Inhibition of transforming growth factor-β production in brain pericytes contributes to cyclosporine A-induced dysfunction of the blood-brain barrier. Cell. Mol. Neurobiol. (in press), 2007

Yamauchi A, Dohgu S, Nishioku T, Shuto H, Naito M, Tsuruo T, Sawada Y, Kataoka Y: An inhibitory role of nitric oxide in the dynamic regulation of the blood-brain barrier function. Cell. Mol. Neurobiol. (in press), 2007

Doh-ura K, Tamura K, Karube Y, Naito M, Tsuruo T, Kataoka Y: Chelating compound, chrysoidine, is more effective in both anti-prion activity and brain endothelial permeability than quinacrine. Cell. Mol. Meurobiol. (in press), 2007

Nishioku T, Takata F, Yamauchi A, Sumi N, Yamamoto I, Fujino A, Naito M, Tsuruo T, Shuto H, Kataoka Y: Protective action of indapamide, a thiazide-like diuretic, on ischemia-induced injury and barrier dysfunction in mouse brain microvascular endothelial cells. J. Phamacol. Sci. (inpress), 2007

2．学会発表

Yamauchi A, Dohgu S, Takata F, Sumi N, Nishioku T, Shuto H, Niwa M, Kataoka Y: Immunosuppressant and blood-brain barrier. Biofunction and Drug Discovery Symposium 2006, September 8-9, 2006, Fukuoka, Japan

H．知的財産権の出願・登録状況

なし

研究成果の刊行に関する一覧表
(2006年4月1日ー2007年3月31日迄)

名前〈片岡　泰文〉

書籍

該当なし

雑誌

発表者氏名	論文タイトル名	発表誌名	巻号	ページ	出版年
Takata F, Dohgu S, Yamauchi A, Sumi N, Nakagawa S, Naito M, Tsuruo T, Shuto H, Kataoka Y	Inhibition of transforming growth factor-β production in brain pericytes contributes to cyclosporine A-induced dysfunction of the blood-brain barrier	Cell Mol Neurobiol			in press
Yamauchi A, Dohgu S, Nishioku T, Shuto H, Naito M, Tsuruo T, Sawada Y, Kataoka Y	An inhibitory role of nitric oxide in the dynamic regulation of the blood-brain barrier function	Cell Mol Neurobiol			in press
Doh-ura K, Tamura K, Karube Y, Naito M, Tsuruo T, Kataoka Y	Chelating compound, chrysoidine, is more effective in both anti-prion activity and brain endothelial permeability than quinacrine	Cell Mol Neurobiol			in press
Nishioku T, Takata F, Yamauchi A, Sumi N, Yamamoto I, Fujino A, Naito M, Tsuruo T, Shuto H, Kataoka Y	Protective action of indapamide, a thiazide-like diuretic, on ischemia-induced injury and barrier dysfunction in mouse brain microvascular endothelial cells	J. Pharmacol. Sci.			in press

分担研究報告書

血液脳関門を介した異物排泄メカニズムにおける薬物間相互作用の予測システムの開発

分担研究者

分担研究者　楠原　洋之　東京大学大学院薬学系研究科　助教授

研究要旨　血液脳関門の異物排泄過程における薬物間相互作用予測システムの構築を目指して研究を行った。血液脳関門に発現するABCトランスポーターBCRPについて、発現系を用いたin vitro輸送実験、ならびにBCRPノックアウトマウスを用いたin vivo実験を行った。ダントロレンを始めとして、BCRPをノックアウトすることにより脳内濃度が増加する化合物を複数見出じた。BCRP発現系を用いて、BCRPの輸送能力をin vitroで測定したところ、in vivoでの脳内濃度の増加とin vitroでの輸送活性の間に明確な相関関係は見られなかった。一方で、同じく血液脳関門に発現するABCトランスポーターであるP-glycoprotein/Mdr1aの輸送能力をin vitroで測定すると、BCRPノックアウトマウスでの脳内薬物濃度の増加とは逆相関を示した。このことは、BCRPとP-gpは重複した基質選択性を示し、BCRP選択的な基質となるものがノックアウトの影響を強く受ける事を示している。今回、BCRPノックアウトマウスでダントロレンの脳内濃度がもっとも大きく増加し、BCRPを介した薬物間相互作用を評価するためのプローブ薬としての有効であるものと考えている。

A.研究目的

血液脳関門の関門機能の破綻には、tight junctionの障害による生理的な破綻と併用薬との薬物間相互作用による異物排泄メカニズムの機能低下による薬物動態学的な破綻の２つの可能性を考慮することが必要である。後者については、キニジンとロペラミドとの薬物間相互作用は血液脳関門を介した異物排泄メカニズムを介したものであることが示唆されている。このような薬物間相互作用を予測・評価するシステムを開発することは、安全な薬剤療法を達成するために必須である。

本研究では、特に後者による関門機能の破綻に焦点をあて、異物排泄に働くトランスポーター（BCRP）に着目し、BCRPによりくみ出される医薬品の探索、ならびにin vitroでのBCRP輸送機能との相関を明らかにすることで、薬物間相互作用の評価系を確立することを目的とした。

B.研究方法

１）マウスに静脈内定速静注を行い、定常状態での血漿中濃度ならびに脳内濃度を測定した。

２）マウス*in situ*脳灌流法を用いて、脳移行性を測定した。

３）MDCK II細胞にBCRPをLLC-PK1細胞にP-gp/Mdr1aをそれぞれ発現させた細胞を多孔性フィルター上に単層培養し、経細胞輸送を測定した。基底膜側から頂側膜方向への経細胞輸送と反対方向への輸送の比をとり、トランスポーターの輸送活性を反映したパラメータとした。

C.研究結果

１）定常状態での脳内薬物濃度の比較により、MeIQx (2.4)、dantrolene (6.3)、flavopiridol (1.7)、prazosin (1.5)、triamterene (2.1)について、脳-血漿濃度比が増加した（カッコ内は増加した比を表す）。

２）定常状態での脳内濃度が増加した化合物について、マウス*in situ*脳灌流法を用いて脳移行性を測定した。その結果、dantrolene、daidzeinについてはBCRPノックアウトマウスで有意に増加していたが、定常状態で観察されたほど大きな変化ではなかった。

３）昨年度報告したPhIPとこれらの化合物、植物エストロジェンについて、単層培養したBCRP発現MDCK II細胞を用いて経細胞輸送について評価した。いずれの化合物も、基底膜側から頂側膜側への経細胞輸送が促進されていた。BCRP発現細胞における基底膜側から頂側膜側、頂側膜側から基底膜側への経細胞輸送の比を非発現細胞での輸送比で除して得られるパラメータをCFR(corrected flux ratio)として、in vivoでの脳-血漿濃度比の増加とプロットしたところ、両者の間に明確な相関は観察されなかった。

P-gp/Mdr1a発現LLC-PK1細胞を用いて、

別紙４

研究成果の刊行に関する一覧表

書籍

著者氏名	論文タイトル名	書籍全体の編集者名	書　籍　名	出版社名	出版地	出版年	ページ

雑誌

発表者氏名	論文タイトル名	発表誌名	巻号	ページ	出版年
Lee Y.J., Maeda J., Kusuhara H., Okauchi T., Inaji M., Nagai Y., Obayashi S., Nakao R., Suzuki K., Sugiyama Y. and Suhara T.	In Vivo Evaluation of P-glycoprotein Function at the Blood-Brain Barrier in Nonhuman Primates Using [11C]Verapamil.	J Pharmacol Exp Ther.	316	647-53	2006
Ikoma Y., Takano A., Ito H., Kusuhara H., Sugiyama Y., Arakawa R., Fukumura T., Nakao R., Suzuki K. and Suhara T.	Quantitative Analysis of 11C-Verapamil Transfer at the Human Blood-Brain Barrier for Evaluation of P-glycoprotein Function.	J Nucl Med.	47	1531-1537	2006
Takano A., Suhara T., Yasuno F., Suzuki K., Takahashi H., Morimoto T., Lee Y.J., Kusuhara H., Sugiyama Y. and Okubo Y.	The antipsychotic sultopride is overdosed - a PET study of drug-induced receptor occupancy in comparison with sulpiride.	Int J Neuropsychopharmacol.	9	539-545	2006

研究成果の刊行に関する一覧表

書籍

小泉修一（2006）グリア細胞によるシナプス伝達制御に関する研究.　ブレインサイエンス・レビュー2006（伊藤正男、川合述史　編）、105-120.

雑誌

発表者氏名	論文タイトル名	発表誌名	巻号	ページ	出版年
Koizumi, S., Shigemoto-Mogami, Y., Nasu-Tada, K., Shinozaki, Y., Ohsawa, K., Tsuda, M., Joshi, B.V., Jacobson, K. A., Kohsaka, S. and Inoue, K	UDP acting at $P2Y_6$ receptors is a novel mediator of microglial phagocytosis.	Nature			in press
Shinozaki, T., Koizumi, S., Ohno, T., Nagao, T. and Inoue, K.	Extracellular ATP countrtacts the ERK1/2-Mediated Death-Promoting Signaling Cascades in Astrosytes	Glia	54	606-618	2006
Tozaki-Saito, H., Koizumi, S., Sato, Y., Tsuda, M., Nagao, T. and Inoue, K.	Retinoic acids increase $P2X_2$ receptor expression through the 5'-flanking region of P2rx2 gene in rat phaeochromocytoma PC12 cells.	Mol. Pharmacol.	319-328	319-328	in press
小泉修一、藤下加代子、津田誠、井上和秀	ATP を介した皮膚ケラチノサイト間情報連絡と痛み	Pain Research	21,	133-139	2006
小泉修一、藤下加代子、津田誠、井上和秀	G 蛋白質共役型 ATP 受容体と痛み	ペインクリニック	27	560-568	2006
Takata F, Dohgu S, Yamauchi A, Sumi N, Nakagawa S, Naito M, Tsuruo T, Shuto H, Kataoka Y	Inhibition of transforming growth factor-β production in brain pericytes contributes to cyclosporine A-induced dysfunction of the blood-brain barrier	Cell Mol Neurobiol			in press
Yamauchi A, Dohgu S, Nishioku T, Shuto H, Naito M, Tsuruo T, Sawada Y, Kataoka Y	An inhibitory role of nitric oxide in the dynamic regulation of the blood-brain barrier function	Cell Mol Neurobiol			in press

発表者氏名	論文タイトル名	発表誌名	巻号	ページ	出版年
Doh-ura K, Tamura K, Karube Y, Naito M, Tsuruo T, Kataoka Y	Chelating compound, chrysoidine, is more effective in both anti-prion activity and brain endothelial permeability than quinacrine	Cell Mol Neurobiol			in press
Nishioku T, Takata F, Yamauchi A, Sumi N, Yamamoto I, Fujino A, Naito M, Tsuruo T, Shuto H, Kataoka Y	Protective action of indapamide, a thiazide-like diuretic, on ischemia-induced injury and barrier dysfunction in mouse brain microvascular endothelial cells	J. Pharmacol. Sci.			in press
Lee Y.J., Maeda J., Kusuhara H., Okauchi T., Inaji M., Nagai Y., Obayashi S., Nakao R., Suzuki K., Sugiyama Y. and Suhara T.	In Vivo Evaluation of P-glycoprotein Function at the Blood-Brain Barrier in Nonhuman Primates Using [11C]Verapamil	J Pharmacol Exp Ther.	316	647-53	2006
Ikoma Y., Takano A., Ito H., Kusuhara H., Sugiyama Y., Arakawa R., Fukumura T., Nakao R., Suzuki K. and Suhara T.	Quantitative Analysis of 11C-Verapamil Transfer at the Human Blood-Brain Barrier for Evaluation of P-glycoprotein Function.	J Nucl Med	47	1531-1537	2006
Takano A., Suhara T., Yasuno F., Suzuki K., Takahashi H., Morimoto T., Lee Y.J., Kusuhara H., Sugiyama Y. and Okubo Y.	The antipsychotic sultopride is overdosed - a PET study of drug-induced receptor occupancy in comparison with sulpiride	Int J Neuropsychopharmacol	9	539-545	2006

doi:10.1038/nature05704

LETTERS

UDP acting at $P2Y_6$ receptors is a mediator of microglial phagocytosis

Schuichi Koizumi[1,2]*, Yukari Shigemoto-Mogami[1]*, Kaoru Nasu-Tada[1], Yoichi Shinozaki[1,3], Keiko Ohsawa[4], Makoto Tsuda[3], Bhalchandra V. Joshi[5], Kenneth A. Jacobson[5], Shinichi Kohsaka[4] & Kazuhide Inoue[3]

Microglia, brain immune cells, engage in the clearance of dead cells or dangerous debris, which is crucial to the maintenance of brain functions. When a neighbouring cell is injured, microglia move rapidly towards it or extend a process to engulf the injured cell. Because cells release or leak ATP when they are stimulated[1,2] or injured[3,4], extracellular nucleotides are thought to be involved in these events. In fact, ATP triggers a dynamic change in the motility of microglia *in vitro*[5,6] and *in vivo*[3,4], a previously unrecognized mechanism underlying microglial chemotaxis[5,6]; in contrast, microglial phagocytosis has received only limited attention. Here we show that microglia express the metabotropic $P2Y_6$ receptor whose activation by endogenous agonist UDP triggers microglial phagocytosis. UDP facilitated the uptake of microspheres in a $P2Y_6$-receptor-dependent manner, which was mimicked by the leakage of endogenous UDP when hippocampal neurons were damaged by kainic acid *in vivo* and *in vitro*. In addition, systemic administration of kainic acid in rats resulted in neuronal cell death in the hippocampal CA1 and CA3 regions, where increases in messenger RNA encoding $P2Y_6$ receptors that colocalized with activated microglia were observed. Thus, the $P2Y_6$ receptor is upregulated when neurons are damaged, and could function as a sensor for phagocytosis by sensing diffusible UDP signals, which is a previously unknown pathophysiological function of P2 receptors in microglia.

Microglia express several functional P2 receptors, and their $P2X_4$, $P2X_7$ and $P2Y_{12}$ receptors have already been described in relation to their physiological and pathophysiological consequences[5–9]. To investigate the expression of mRNAs for P2 receptors that are at a higher concentration in cultured rat microglia, we conducted reverse-transcriptase-mediated polymerase chain reaction (RT–PCR) analysis with complementary DNA coding for P2Y and P2X receptors (Fig. 1a). In accordance with previous reports[5–9], microglia expressed mRNAs encoding $P2X_4$, $P2X_7$ and $P2Y_{12}$ receptors. However, we found unexpectedly that cultured rat microglia expressed a large amount of mRNA coding for $P2Y_6$ receptors, which was also confirmed by western blotting for the expression of $P2Y_6$ receptor protein (Fig. 1b). The $P2Y_6$ receptor is coupled to the activation of phospholipase C (PLC), leading to the production of inositol 1,4,5-trisphosphate ($InsP_3$) and the release of Ca^{2+} from $InsP_3$-receptor-sensitive stores[10,11]. We therefore examined changes in the intracellular Ca^{2+} concentration ($[Ca^{2+}]_i$) in microglia and found that the $P2Y_6$ receptor agonist UDP evoked increases in $[Ca^{2+}]_i$ in a concentration-dependent manner, and it also increased the fraction of the UDP-responsive cells (Supplementary Fig. 1a). The elevations in $[Ca^{2+}]_i$ induced by 100 μM UDP were significantly inhibited by the PLC inhibitor U73122, the Ca^{2+}-ATPase inhibitor in sarcoplasmic/endoplasmic reticulum thapsigargin, and the membrane-permeable $InsP_3$ receptor inhibitor xestospongin C, but were little affected by pertussis toxin (Supplementary Fig. 1b). The UDP-evoked $[Ca^{2+}]_i$ increases in microglia were significantly inhibited by reactive blue 2 (RB2), known as a potent $P2Y_6$ antagonist[11], suramin, which inhibits $P2Y_6$ receptor at higher concentrations, the diisothiocyanate derivative MRS2578, which is a selective antagonist of the $P2Y_6$ receptor[12], and an antisense oligonucleotide (AS) for $P2Y_6$ receptors, but not by a random-sequence oligonucleotide (R-oligo) (Fig. 1c). All these data show that rat microglia express functional $P2Y_6$ receptors by which UDP mobilizes Ca^{2+}.

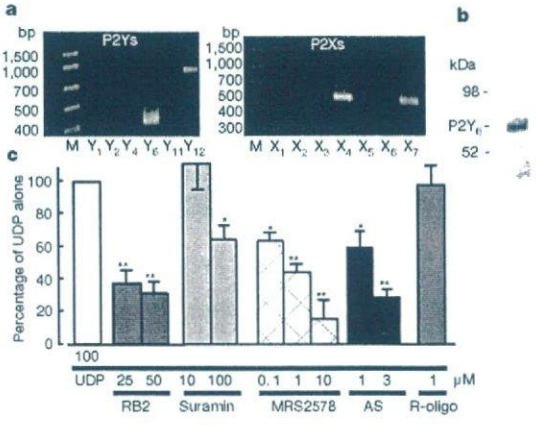

Figure 1 | Expression of $P2Y_6$ receptor and UDP-evoked increase in $[Ca^{2+}]_i$ in cultured microglia. a, RT–PCR analysis of the expression of mRNAs for $P2Y_6$, $P2Y_{12}$, $P2X_4$ and $P2X_7$ receptors in microglial cells. **b**, Expression of $P2Y_6$ receptor protein confirmed by western blotting analysis. **c**, Effects of various chemicals on the increase in $[Ca^{2+}]_i$ (measured as the change in ratio of fluorescence at 340 nm to that at 380 nm) evoked by 100 μM UDP in microglia. The maximum increase in Fura-2 fluorescence evoked by 100 μM UDP was considered as the control response, and values are expressed as a percentage of control. Data show means and s.e.m. for 24–36 cells obtained from at least three independent experiments. Significant differences from the response to UDP alone: asterisk, $P < 0.05$; two asterisks, $P < 0.01$ (Student's *t*-test).

[1]Division of Pharmacology, National Institute of Health Sciences, 1-18-1 Kamiyoga, Setagaya, Tokyo 158-8501, Japan. [2]Department of Pharmacology, Interdisciplinary Graduate School of Medicine and Engineering, University of Yamanashi, 1110 Shimokato, Chuo, Yamanashi 409-3893, Japan. [3]Department of Molecular and System Pharmacology, Graduate School of Pharmaceutical Sciences, Kyushu University, 3-1-1 Maidashi, Higashi, Fukuoka 812-8582, Japan. [4]Department of Neurochemistry, National Institute of Neuroscience, 4-1-1 Ogawahigashi, Kodaira, Tokyo 187-8502, Japan. [5]Molecular Recognition Section, Laboratory of Bioorganic Chemistry, National Institute of Diabetes and Digestive and Kidney Diseases, National Institutes of Health, Bethesda, Maryland 20892-0810, USA.
*These authors contributed equally to this work

Morphogenesis, cell movement and phagocytosis are driven by dynamic reorganization of the actin cytoskeleton[13,14]. We showed previously that activation of $P2Y_{12/13}$ receptors, another microglial G-protein-coupled receptor, resulted in membrane ruffling and chemotaxis in microglia[5,6], and therefore we sought first to determine whether the $P2Y_6$-receptor-mediated signals affect the cell movement of microglia. Membrane ruffles are structures that are found primarily at the front edges of migrating cells[15]. To determine whether $P2Y_6$ activation stimulates microglial chemotaxis, cells were stimulated with either UDP or ATP. Neither lamellipodia-like membrane ruffles (Fig. 2a left) nor chemotaxis (Fig. 2b left) were observed when stimulated with UDP, whereas ATP produced both responses (Fig. 2a right and Fig. 2b right). However, UDP caused actin reorganization and formed aggregates of F-actin in the interior of the cells (Fig. 2a left, arrows). On stimulation with UDP (100 μM), microglia rapidly changed their morphology (Supplementary Fig. 2a); namely, to microglial processes with filopodia-like protrusions (arrows) and phagosome-like vacuoles (arrowheads). A crown-like circular structure rich in F-actins, termed the 'phagocytotic cup'[16], was also observed around the zymosan particles (Supplementary Fig. 2b, red). We speculated that UDP somehow regulates the morphogenesis of microglia, which may be involved in microglial endocytotic activities such as pinocytosis, macropinocytosis and phagocytosis. Phagocytosis is one of the most important physiological functions of microglia[17] and is the process activating the uptake of larger particles (more than 0.5 μm) by actin-based mechanisms. We investigated the UDP-evoked phagocytosis process by time-lapse videomicroscopy and flow cytometry (fluorescence-activated cell sorting; FACS)-based assay. When stimulated with 100 μM UDP, microglia rapidly phagocytosed fluorescent zymosan particles (green) (Fig. 2c, see also Supplementary Video). A quantitative phagocytosis assay by FACS shows that UDP induced the phagocytosis of latex beads in a concentration-dependent fashion (5–1,000 μM) in a 20-min incubation period (Fig. 2d). GDP (100–1,000 μM), a weak agonist of the $P2Y_6$ receptor, caused a slight uptake of microspheres (at 100 μM this was 49.7 ± 8.6% of UDP alone; $n = 4$) but ADP, also known as a weak partial agonist of the mouse $P2Y_6$ receptor, failed to stimulate the uptake (at 100 μM it was 0.3 ± 2.3% of UDP alone; $n = 4$). This is in good agreement with the previous finding that ADP does not activate rat $P2Y_6$ receptors[18]. The phagocytosis induced by 100 μM UDP was significantly inhibited by 30–100 μM RB2, a higher concentration of suramin (300 μM) and MRS2578 (0.01–3 μM), and was nearly abolished by $P2Y_6$ AS (Fig. 2e; see also Supplementary Fig. 2c, d). Recent reports indicate the existence of functional cross-talk between the nucleotides and cysteinyl leukotrienes (CysLTs, for example LTD4) in orchestrating inflammatory responses[19], indicating that some nucleotides may reveal their functions by means of a CysLT receptor (CysLTR). Microglia express a functional CysLT1R, whose activation by LTD4 resulted in an increase in $[Ca^{2+}]_i$ in microglia (Supplementary Fig. 3a). Thus, UDP acting on CysLT1R may reveal various microglial responses. However, MRS2578, a selective $P2Y_6$ receptor antagonist, did not block the LTD4-evoked Ca^{2+} responses in CysLT1R-transfected Chinese hamster ovary cells (Supplementary Fig. 3b) at a dose that inhibited the UDP-evoked increase in $[Ca^{2+}]_i$ and phagocytosis in microglia (Figs 1c and 2e). In addition, 1 μM LTD4 did not induce phagocytosis in microglia (Supplementary Fig. 3c, 4.8 ± 4.2% of that with 100 μM UDP alone; $n = 3$). All these findings suggest that the contribution of the CysLT1R to the UDP-evoked phagocytosis in microglia is negligible. Taken together, these data strongly suggest that rat microglial $P2Y_6$ receptors are coupled with phagocytic functions. The UDP-evoked phagocytosis was inhibited by 1 μM thapsigargin, the protein kinase C inhibitor staurosporin at 5 μM, and 10 μM U73122 (see Supplementary Fig. 4), indicating that activation of the $P2Y_6$ receptor seems to trigger phagocytosis through the pathway(s) mediated by PLC-linked Ca^{2+} and protein kinase C.

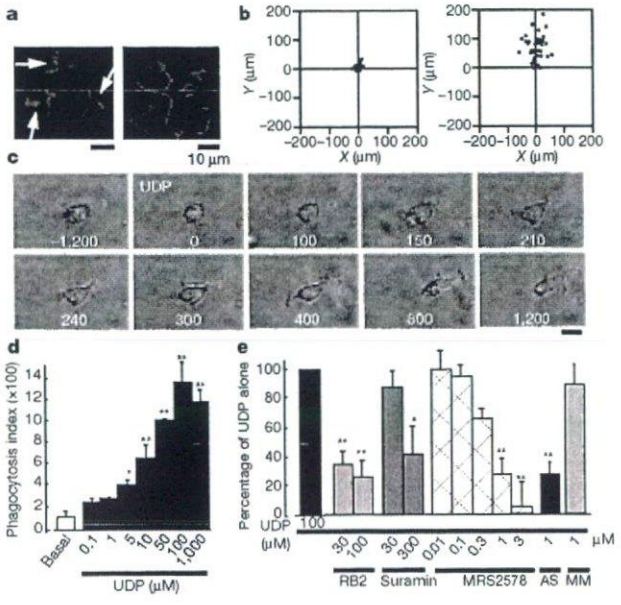

Figure 2 | Changes in cell motilities of microglia. **a**, UDP- and ATP-evoked membrane ruffles. Cultured microglia were stimulated for 5 min with 100 μM UDP (left) and 10 μM ATP (right), fixed, permeabilized, and then stained with anti-phalloidin. Scale bar, 10 μm. **b**, Typical chemotactic responses of microglia towards 100 μM UDP (left) and 100 μM ATP (right) assessed by the Dunn chemotaxis chamber (see Methods). **c**, Time-lapse images showing the effect of UDP on the microglial morphogenic changes and the uptake of fluorescent zymosan particles (green). The time after addition of UDP is shown in seconds in each picture. **d**, The UDP-evoked uptake of microspheres was assessed quantitatively as a phagocytosis index by using FACS. Data are mean and s.e.m. for three experiments (asterisk, $P < 0.05$; two asterisks, $P < 0.01$ compared with basal). **e**, Effects of the P2 receptor antagonists reactive blue 2 and suramin, the $P2Y_6$ receptor antagonist MRS2578, and $P2Y_6$ AS or MM on the UDP-evoked phagocytosis. Data are means and s.e.m. for three or four experiments (asterisk, $P < 0.05$; two asterisks, $P < 0.01$ compared with UDP alone).

Because phagocytes remove dead or damaged cells, debris and invading pathogens, recognition is the first step in phagocytosis. It is initiated by activation of the phagocytosis-promoting receptors such as Fc receptors and complement receptors[20]. In the central nervous system, microglia possess these receptors and remove amyloid-β, a key molecule in Alzheimer's disease, and attenuate Alzheimer's disease-like pathology[21]. With regard to apoptotic cells, microglia may also remove such cells by recognizing so-called 'eat-me' signals[20]. However, in the present study we used non-opsonized zymosan (Fig. 2c) and latex beads (Fig. 2d, e), which were not recognized by opsonin-dependent receptors such as Fc receptors, complement receptors or vitronectin receptors. Phagocytosis-promoting receptors also include opsonin-independent ones such as β_1-integrins, mannose receptors, scavenger receptors and phosphatidylserine receptors[13]; in fact, microglia expressed all these receptors (Supplementary Fig. 5a–e, cell lysates). Among these receptors, β_1-integrin was detected as a bead-associated protein that was slightly increased on stimulation with UDP (Supplementary Fig. 5a, bead-associated) and localized at membrane ruffle-like or phagocytic cup-like structures (see also Supplementary Fig. 2b), to which fluorescent microspheres were attached (Supplementary Fig. 5f). However, we do not know whether β_1-integrin itself binds or recognizes the microspheres. β_1-Integrin might be involved in some way in the machinery of phagocytosis or in the uptake processes of the microspheres in response to UDP, but the precise target molecule or molecules that bind or recognize microspheres to be phagocytosed remains to be identified. The microglial phagocytosis seen in the present study is a new type that is promoted by the diffusible

extracellular molecule UDP. However, we cannot deny the possibility that the UDP may simply facilitate the machinery of phagocytosis and that UDP-evoked phagocytosis observed in this study may even include macropinocytosis.

To determine the expression and function of microglial $P2Y_6$ receptors *in vivo*, the excitotoxicity of brain injury was induced by kainic acid (KA) (Fig. 3). KA is an excitatory amino acid that is often used to cause limbic motor epilepsy or excitatory neuronal cell death *in vivo* and *in vitro*. KA acts on non-NMDA glutamate receptors to facilitate excess excitability, thereby leading to necrosis and even apoptosis of neurons. The hippocampal CA1 and CA3 regions are susceptible to neuronal death in response to KA[22]. When KA was injected intraperitoneally into rats ($10\,mg\,kg^{-1}$), it produced typical limbic seizure within 60 min. At 72 h after the administration of KA, the brains were removed and were used for western blotting, immunohistochemical assays and *in situ* hybridization (ISH). Western blotting analysis showed that KA increased the expression of $P2Y_6$ receptors in comparison with the saline-injected control groups (Fig. 3A, B). Double staining of microglia and neurons by anti-Iba1 (green) and anti-neuronal nuclei (NeuN, red) antibodies, respectively, showed that KA induced severe neuronal loss in the hippocampal CA1 and CA3 regions, where intense Iba1-positive signals—indicative of microglia—were observed. KA increased the number of microglia appearing in the activated form with poorly ramified, short and thick processes (Fig. 3C, f–h). Small NeuN signals seemed to be incorporated in some microglia (see g and h in Fig. 3C), suggesting that microglia phagocytose damaged or dead neurons. These findings suggest that microglia might migrate or proliferate, probably as a result of KA-induced neuronal damage.

We further examined the cell types that produced increases in $P2Y_6$ receptor protein in response to the administration of KA, and found that $P2Y_6$ immunoreactivities (green in Fig. 3D) were associated with the microglia (OX-42, red in Fig. 3D, c) but not with astrocytes (glial fibrillary acidic protein (GFAP), red in Fig. 3D, d) or neurons (NeuN, red in Fig. 3D, e). Furthermore, we performed ISH to characterize the expression of mRNA coding for $P2Y_6$ receptors with the use of digoxigenin-labelled antisense RNA probe. Signals for $P2Y_6$ receptor mRNA were very low in the naive animals but were upregulated three days after treatment with KA (Fig. 3E, b; blue dots indicated by arrowheads). At this time, the number of microglia increased markedly, especially at the hippocampal CA3 and CA1 regions (Fig. 3C). After ISH, the sections were stained with anti-Iba1 antibody to characterize $P2Y_6$ receptor mRNA signals. In the hippocampal CA3 regions of naive rats, there were very few anti-Iba1-positive microglia that did not show $P2Y_6$ receptor mRNA. In contrast, in the hippocampal CA3 of KA-injected rats, there was an increased number of anti-Iba1-positive microglia, in which $P2Y_6$ receptor signals were colocalized with microglia (Fig. 3E, c; KA, black arrows, see also inset at higher magnification).

There is a growing literature about 'eat-me' signals that are expressed on the cell surface of apoptotic or dying cells. However, diffusible signals that trigger phagocytosis have received only limited attention. When neurons or cells are exposed to traumatic injury such as ischaemia, they swell and subsequently shrink as a result of

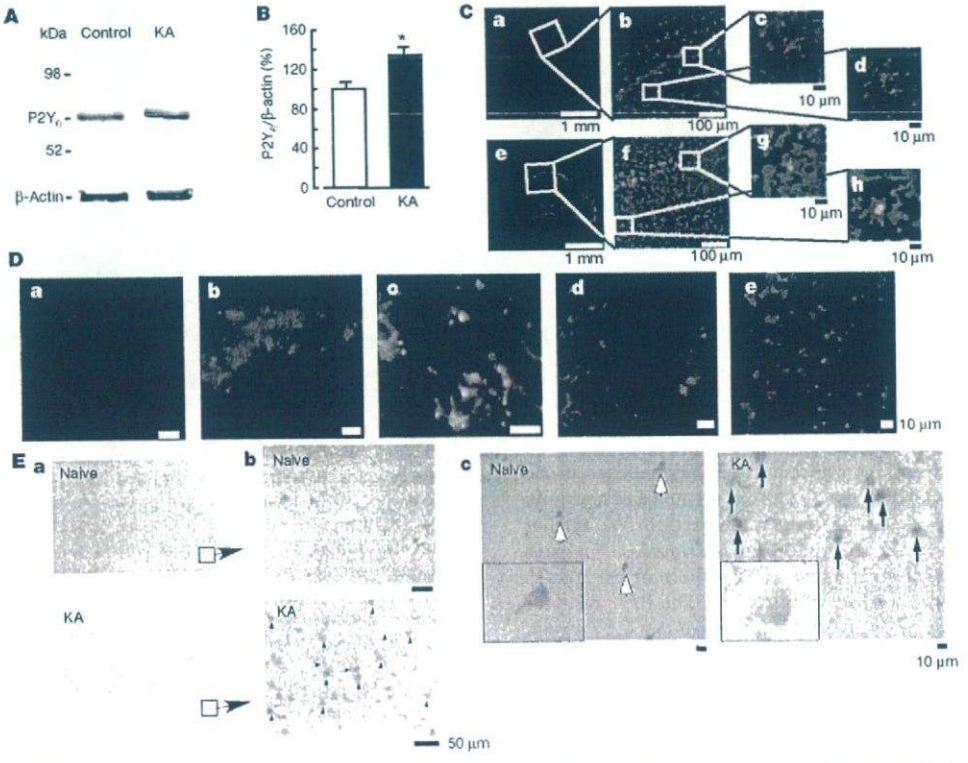

Figure 3 | Increase in $P2Y_6$ receptors in the hippocampus after kainic acid (KA)-treatment. A, Western blot analysis, showing increase in $P2Y_6$ receptor protein in rats treated intraperitoneally with $10\,mg\,kg^{-1}$ KA, 72 h after treatment. **B**, Summary of quantitative data; KA was applied at $10\,mg\,kg^{-1}$. Results are means and s.e.m. for 8 (control) and 7 (KA) experiments (asterisk, $P < 0.05$ compared with control). **C**, Immunohistochemical analysis in naive control (**a**–**d**) and KA-treated (**e**–**h**) rats; red, anti-NeuN antibody; green, anti-Iba1 antibody. Rectangles in **a** and **e** are expanded in **b** and **f**, respectively. Rectangles in **b** and **f** also correspond to **c**, **d** and **g**, **h**, respectively. **D**, Anti-$P2Y_6$ antibody signals (green) were increased by KA (**a**, control; **b**, KA), which was colocalized with microglia (red in **c**, anti-OX42) but not with astrocytes (red in **d**, anti-GFAP) or neurons (red in **e**, anti-NeuN). **E**, ISH analysis. **a**, **b**, mRNA coding for $P2Y_6$ receptor in naive rats was very low but was increased at the hippocampal CA3 region by KA (3 days later) (blue dots and arrowheads, KA). **c**, Double staining with $P2Y_6$ antisense RNA probe (blue dots) and anti-Iba-1 antibody (brown signals, white (naive) or black (KA) arrows). In KA-treated rats there was an increased number of microglia, which was associated with $P2Y_6$ receptor mRNA (blue signals, inset at higher magnification in KA).

increased permeability. This is followed by leakage of cytoplasmic molecules, leading to necrotic cell death. Thus, cytoplasmic nucleotides could be diffusible messengers that signal the crisis state to adjacent cells including microglia. In fact, the diffusible messenger ATP promotes microglial chemotaxis and/or migration[3–6]. Diffusible molecules might be insufficiently precise to cause phagocytes to recognize and eat cells. However, released or leaked nucleotides are immediately degraded by the extracellular nucleotide-degrading enzymes. In this respect, UDP might be a localized and transient marker of traumatized or necrotic cells.

Cell injury results in a leakage of ATP that affects the motility of adjacent cells, including microglia[3,4]. In addition, cells release or leak uridine nucleotides[23] and nucleotide sugars[24] in response to various stimuli or ischaemic injury[25]. We therefore next investigated whether KA increases the release of extracellular UDP from neurons to induce microglial phagocytosis. Cultured hippocampal neurons were stimulated with and without 100 μM KA for 1 h; the supernatant was then collected for nucleotide assay by high-performance liquid chromatography (HPLC) or for phagocytosis assay by FACS (Fig. 4). Because released or leaked UTP is rapidly degraded into UDP, UMP and uridine by ARL67156-sensitive ectonucleotidases, we monitored the amount of UTP rather than UDP, and collected the supernatant and the microdialysates in the presence of 20 μM ARL67156 throughout experiments. There was a close relationship between the HPLC peak corresponding to UTP and the concentration of the standard UTP ($R^2 = 0.9947$). The amount of UTP in the KA-treated supernatant was significantly larger than that in the KA-untreated control supernatant (Fig. 4b; control, 2.3 ± 1.1 μM; KA treated, 10.5 ± 3.9 μM, $P < 0.05$). We also tested whether the KA-treated supernatant obtained from cultured hippocampal neurons facilitated microglial phagocytosis. Hippocampal neurons were treated with and without 100 μM KA for 1 h; each supernatant was collected and added to microglia; this was followed by a phagocytosis assay. As shown in Fig. 4c, when microglia were incubated with the KA-treated supernatant for 20 min, there was a significant increase in phagocytosis, which was blocked by the $P2Y_6$ receptor antagonist MRS2578 (1 μM). KA alone did not stimulate phagocytosis.

Finally, we tested whether KA induces the release of UDP and $P2Y_6$-receptor-mediated phagocytosis *in vivo*. An increase in extracellular UTP concentration ($[UTP]_o$) was observed soon after injection of KA (from 1 to 4 h after injection), which reached 2–3-fold higher than the KA-untreated control (data not shown). At 1 day after KA injection, $[UTP]_o$ was about 1.5–2.0-fold higher than the KA-untreated control (Fig. 4e). Then, at day 3, $[UTP]_o$ reached almost 10-fold higher levels (9.4 ± 1.2-fold; Fig. 4e and inset), which decreased slightly at day 5. A higher (5–10-fold) $[UTP]_o$ was observed 2–3 days after the injection of KA, which lasted at least another couple of days. It should be noted that loss of neurons (removal of neurons) also became obvious 2–3 days after the KA injection. We further injected fluorescent microspheres into the hippocampal CA3 regions of KA-treated rats, and then counted the numbers of the microspheres phagocytosed or attached by microglia. The $P2Y_6$ receptor antagonist MRS2578 was injected into the hippocampal CA3 region, and $P2Y_6$ AS or MM (mismatch oligonucleotide) was injected into the third ventricle. The number of microspheres taken or attached by microglia was markedly increased by KA treatment, which is significantly inhibited by MRS2578 or $P2Y_6$ AS but not by MM (Fig. 4g; see also Supplementary Fig. 6). These findings all suggest that UDP/$P2Y_6$-receptor-mediated signals are important for microglial phagocytosis even *in vivo*.

A recent review described that dying cells use both 'find-me' and 'eat-me' signals for phagocyte attraction and recognition[26]. Nucleotides could be both 'find-me' and 'eat-me' signals. The intracellular ATP concentration is estimated to be high (more than 5 mM) and the UTP concentration is reported to be one-third that of ATP[23]. Cells release ATP, and here we showed that KA caused an increase in extracellular UTP or UDP. Microglia might therefore be attracted by ATP or ADP[5,6] and subsequently recognize UDP, leading to the removal of the dying cells or their debris. It is interesting that ATP/ADP is not able to efficiently activate $P2Y_6$ receptors; neither can UDP act on $P2Y_{12/13}$ receptors. Thus, even if these nucleotides were leaked or released simultaneously, adenine and uridine nucleotides would regulate microglial motilities, namely chemotaxis and phagocytosis, in a mutually exclusive but coordinated fashion.

So far we have not shown quantitative data indicating that individual microglia upregulate the expression of $P2Y_6$ receptors. A significant, but not drastic, increase in $P2Y_6$ receptor protein in the hippocampus was observed after injection of KA (Fig. 3A, B). ISH data show that expression of mRNA coding for $P2Y_6$ receptors in microglia was very low in naive animals but became obvious in an increased number of microglia after KA injection (Fig. 3E), suggesting that the increase in $P2Y_6$ receptor protein is not due simply to an increased number of microglia but is upregulated in individual

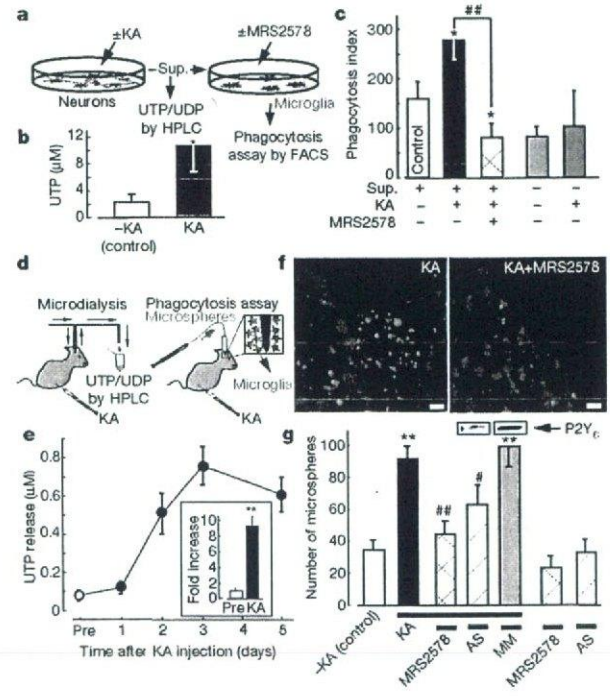

Figure 4 | KA-evoked increases in extracellular uridine nucleotides and $P2Y_6$-receptor-mediated microglial phagocytosis *in vitro* and *in vivo*. **a**, Schematic diagram of the experiments *in vitro*. Sup., supernatant. **b**, Summary of the UTP concentration in the KA-treated and control supernatants. Data show means and s.e.m. for at least five independent experiments (asterisk, $P < 0.05$ compared with control). **c**, Effects of the KA-treated and control supernatant on microglial uptake of fluorescent latex beads. Data show means and s.e.m. for at least four independent experiments (asterisk, $P < 0.05$ compared with control; hash sign, $P < 0.05$ compared with KA-treated supernatant). **d**, Schematic diagram of the experiments *in vivo*. KA was applied intraperitoneally at 10 mg kg^{-1}. **e**, Time course of changes in $[UTP]_o$ in baseline dialysates (before treatment with KA (Pre), and 1, 2, 3 and 5 days afterwards). Inset, fold increase at day 3 (compared with before treatment). **f**, Typical pictures of fluorescent microspheres (green) attached or taken up by microglia (red, anti-Iba1) in the KA-treated (left) and KA + MRS2578-treated (right) hippocampal CA3 regions. Scale bar, 20 μm. **g**, Quantitative analysis of phagocytosis *in vivo* (details are provided in Supplementary Methods). Changes in $P2Y_6$ receptor protein by $P2Y_6$ AS or MM are shown at the top of corresponding columns. Values are means and s.e.m. (asterisk, $P < 0.01$ compared with control (−KA); hash sign, $P < 0.05$; two hash signs, $P < 0.01$ compared with KA-treated group). Statistical analyses were performed by ANOVA with Scheffe's multiple comparison. At least three sections containing the injection sites were analysed per animal, and at least three animals were used in each group for analysis.

microglia. We also emphasize that even if the extent of $P2Y_6$ receptor upregulation is not drastic, an increase in extracellular UDP, a ligand for $P2Y_6$ receptor, is markedly increased after treatment with KA (detected as UTP, almost 10-fold; Fig. 4e) and therefore that the UDP/$P2Y_6$ receptor system would be sufficiently activated to cause microglial phagocytosis after treatment with KA. In comparison with the extensive knowledge of the molecular events involved in the regulation of apoptosis or necrosis, relatively little is known about the processes responsible for the clearance of dead cells and the degradation of waste materials. Considering the present findings that injured neurons leak diffusible UTP/UDP and cause the upregulation of $P2Y_6$ receptors in microglia, the UDP/$P2Y_6$ receptor system might function as a critical device covering the phagocytosis of both apoptotic and necrotic cells if they release or leak UDP by sensing diffusible UDP signals.

Thus we have shown that microglia express $P2Y_6$ receptors that function as a sensor of phagocytosis. The $P2Y_6$ receptor agonist UDP is released (as UTP) when neurons are damaged by KA. Thus, the activation of $P2Y_6$ receptors by UDP would be a key event in initiating the clearance of dying cells or debris in the central nervous system.

METHODS

Detailed methods are provided in Supplementary Information.

Microglia culture. The protocol was reviewed and approved by the Committee for Institutional Laboratory Animal Care of the National Institute of Health Sciences. Rat primary cultured microglia were prepared in accordance with the method described previously[27].

Phagocytosis assay *in vitro* and *in vivo*. *In vitro* microglial phagocytosis was assessed by either FACScan analysis or imaging analysis with fluorescently labelled microspheres. For the *in vivo* phagocytosis assay, fluorescently labelled microspheres were injected into the hippocampal CA3 region after injection of KA, and then the number of fluorescent microspheres associated with microglia was analysed by confocal microscopy (LSM 5 Pascal; Carl Zeiss).

Microdialysis. A microdialysis probe (A-I type probe; Eicom) was inserted into the hippocampal CA3 region by means of a guide cannula, and was perfused continuously at a flow rate of 3.0 $\mu l\ min^{-1}$ (collected for 60 min) supplemented with the ectonuclease inhibitor ARL67156 (20 μM) (Sigma).

Quantification of UTP by HPLC. The concentration of nucleotides in the supernatant of the hippocampal cultures was analysed with an HPLC system (Jasco) combined with a C_{18} column (4.6 × 250 mm, Shodex) as described[28], with minor modifications.

Data analysis and statistics. All results are expressed as means ± s.e.m. A statistical analysis was performed with Student's *t*-test or analysis of variance, followed by Scheffe's multiple comparison test. Differences were considered to be significant at $P < 0.05$.

Received 23 December 2006; accepted 23 February 2007.
Published online 4 April 2007.

1. Guthrie, P. B. *et al.* ATP released from astrocytes mediates glial calcium waves. *J. Neurosci.* 19, 520–528 (1999).
2. Koizumi, S., Fujishita, K., Tsuda, M., Shigemoto-Mogami, Y. & Inoue, K. Dynamic inhibition of excitatory synaptic transmission by astrocyte-derived ATP in hippocampal cultures. *Proc. Natl Acad. Sci. USA* 100, 11023–11028 (2003).
3. Nimmerjahn, A., Kirchhoff, F. & Helmchen, F. Resting microglial cells are highly dynamic surveillants of brain parenchyma *in vivo*. *Science* 308, 1314–1318 (2005).
4. Davalos, D. *et al.* ATP mediates rapid microglial response to local brain injury *in vivo*. *Nature Neurosci.* 8, 752–758 (2005).
5. Honda, S. *et al.* Extracellular ATP or ADP induce chemotaxis of cultured microglia through $G_{i/o}$-coupled P2Y receptors. *J. Neurosci.* 21, 1975–1982 (2001).
6. Nasu-Tada, K., Koizumi, S. & Inoue, K. Involvement of β1 integrin in microglial chemotaxis and proliferation on fibronectin: different regulations by ADP through PKA. *Glia* 52, 98–107 (2005).
7. Ferrari, D. *et al.* P2Z purinoreceptor ligation induces activation of caspases with distinct roles in apoptotic and necrotic alterations of cell death. *FEBS Lett.* 447, 71–75 (1999).
8. Suzuki, T. *et al.* Production and release of neuroprotective tumor necrosis factor by P2X7 receptor-activated microglia. *J. Neurosci.* 24, 1–7 (2004).
9. Tsuda, M. *et al.* P2X4 receptors induced in spinal microglia gate tactile allodynia after nerve injury. *Nature* 424, 778–783 (2003).
10. Chang, K., Hanaoka, K., Kumada, M. & Takuwa, Y. Molecular cloning and functional analysis of a novel P2 nucleotide receptor. *J. Biol. Chem.* 270, 26152–26158 (1995).
11. Communi, D., Parmentier, M. & Boeynaems, J. M. Cloning, functional expression and tissue distribution of the human P2Y6 receptor. *Biochem. Biophys. Res. Commun.* 222, 303–308 (1996).
12. Mamedova, L. K., Joshi, B. V., Gao, Z. G., von Kugelgen, I. & Jacobson, K. A. Diisothiocyanate derivatives as potent, insurmountable antagonists of P2Y6 nucleotide receptors. *Biochem. Pharmacol.* 67, 1763–1770 (2004).
13. Greenberg, S. Signal transduction of phagocytosis. *Trends Cell Biol.* 5, 93–99 (1995).
14. Mitchison, T. J. & Cramer, L. P. Actin-based cell motility and cell locomotion. *Cell* 84, 371–379 (1996).
15. Lauffenburger, D. A. & Horwitz, A. F. Cell migration: a physically integrated molecular process. *Cell* 84, 359–369 (1996).
16. Ohsawa, K., Imai, Y., Kanazawa, H., Sasaki, Y. & Kohsaka, S. Involvement of Iba1 in membrane ruffling and phagocytosis of macrophages/microglia. *J. Cell Sci.* 113, 3073–3084 (2000).
17. Kreutzberg, G. W. Microglia: a sensor for pathological events in the CNS. *Trends Neurosci.* 19, 312–318 (1996).
18. Nicholas, R. A. *et al.* Pharmacological and second messenger signalling selectivities of cloned P2Y receptors. *J. Auton. Pharmacol.* 16, 319–323 (1996).
19. Mellor, E. A., Maekawa, A., Austen, K. F. & Boyce, J. A. Cysteinyl leukotriene receptor 1 is also a pyrimidinergic receptor and is expressed by human mast cells. *Proc. Natl Acad. Sci. USA* 98, 7964–7969 (2001).
20. Lauber, K. *et al.* Apoptotic cells induce migration of phagocytes via caspase-3-mediated release of a lipid attraction signal. *Cell* 113, 717–730 (2003).
21. Bard, F. *et al.* Peripherally administered antibodies against amyloid β-peptide enter the central nervous system and reduce pathology in a mouse model of Alzheimer disease. *Nature Med.* 6, 916–919 (2000).
22. Sperk, G. *et al.* Kainic acid induced seizures: neurochemical and histopathological changes. *Neuroscience* 10, 1301–1315 (1983).
23. Lazarowski, E. R., Homolya, L., Boucher, R. C. & Harden, T. K. Direct demonstration of mechanically induced release of cellular UTP and its implication for uridine nucleotide receptor activation. *J. Biol. Chem.* 272, 24348–24354 (1997).
24. Lazarowski, E. R., Shea, D. A., Boucher, R. C. & Harden, T. K. Release of cellular UDP-glucose as a potential extracellular signaling molecule. *Mol. Pharmacol.* 63, 1190–1197 (2003).
25. Erlinge, D. *et al.* Uridine triphosphate (UTP) is released during cardiac ischemia. *Int. J. Cardiol.* 100, 427–433 (2005).
26. Ravichandran, K. S. 'Recruitment signals' from apoptotic cells: invitation to a quiet meal. *Cell* 113, 817–820 (2003).
27. Nakajima, K. *et al.* Identification of elastase as a secretory protease from cultured rat microglia. *J. Neurochem.* 58, 1401–1408 (1992).
28. Lazarowski, E. R., Boucher, R. C. & Harden, T. K. Constitutive release of ATP and evidence for major contribution of ecto-nucleotide pyrophosphatase and nucleoside diphosphokinase to extracellular nucleotide concentrations. *J. Biol. Chem.* 275, 31061–31068 (2000).

Supplementary Information is linked to the online version of the paper at www.nature.com/nature.

Acknowledgements We thank T. Shimizu and Dr. S. Ishii for providing CysLT1 receptor-expressed Chinese hamster ovary cells; K. Sakemi for technical assistance; Y. Sasaki for helpful suggestions; K. Suzuki and R. Adachi for allowing us to use the Pascal confocal microscope system; and T. Nishimaki-Mogami, Y. Ohno and T. Nagao for continuous encouragement. This study was supported in part by a grant from The National Institute of Biomedical Innovation, a grant from Uehara Memorial Foundation, a Grant-in-Aid for Scientific Research on Priority Areas, for Creative Scientific Research, Scientific Research (A and B), and for Young Scientists (A) from the Ministry of Education, Science, Sports and Culture of Japan.

Author Contributions S.K. designed most experiments, performed Ca^{2+} imaging and *in vivo* experiments and wrote the paper. Y.S.M. conducted major parts of the experiments. K.N.T. and Y.S. carried out the FACS assay and the HPLC analysis, respectively. K.O. and S.K. performed the chemotaxis analysis. B.V.J. and K.A.J. made the $P2Y_6$ receptor antagonist MRS2578. M.T. analysed the data. K.I. analysed the data and coordinated the project. K.I. also designed the project. All authors discussed the results and commented on the manuscript.

Author Information Reprints and permissions information is available at www.nature.com/reprints. The authors declare no competing financial interests. Correspondence and requests for materials should be addressed to K.I. (inoue@phar.kyushu-u.ac.jp).

GLIA 54:606–618 (2006)

Extracellular ATP Counteracts the ERK1/2-Mediated Death-Promoting Signaling Cascades in Astrocytes

YOUICHI SHINOZAKI,[1] SCHUICHI KOIZUMI,[1] YASUO OHNO,[2] TAKU NAGAO,[2] AND KAZUHIDE INOUE[3]*
[1]*Division of Pharmacology, National Institute of Health Sciences, Setagaya, Tokyo 158-8501, Japan*
[2]*National Institute of Health Sciences, Setagaya, Tokyo 158-8501, Japan*
[3]*Department of Molecular and System Pharmacology, Graduate School of Pharmaceutical Sciences, Kyushu University, Higashi-ku, Fukuoka 812-8582, Japan*

KEY WORDS
purinergic receptor; oxidative stress; ERK1/2; src family; protein tyrosine phosphatase

ABSTRACT
Oxidative stress is the main cause of neuronal death in pathological conditions. Hydrogen peroxide (H_2O_2), one of the reactive oxygen species, activates many intracellular signaling cascades including src family and mitogen-activated protein kinases (MAPKs), some of which are critically involved in the induction of cellular damage. We previously showed that H_2O_2-induced cell death in astrocytes and adenosine 5′-triphosphate (ATP), acting on $P2Y_1$ receptors, had a protective effect. Here, we examined the H_2O_2-induced changes in intracellular signaling cascades that promote cell death in astrocytes, showing the molecular mechanisms by which the activation of $P2Y_1$ receptors counteracts such signals. Although H_2O_2 activated three MAPKs including ERK1/2, p38, and JNK, only the activation of ERK1/2 participated in the H_2O_2-evoked cell death. H_2O_2 induced a sustained activation of ERK1/2 mainly in the nucleus region, which was well in accordance with the H_2O_2-induced cell death. H_2O_2 also activated the src tyrosine kinase family, which was an upstream signal for ERK1/2. Activation of $P2Y_1$ receptors by 2methylthio-ADP (2MeSADP) inhibited the H_2O_2-evoked activation of src tyrosine kinase, resulting in the inhibition of the phosphorylated-ERK1/2 accumulation in the nucleus. 2MeSADP enhanced the gene expression and activity of protein tyrosine phosphatase (PTP), which was responsible for the inhibition of src tyrosine kinase. Thioredoxin reductase, another cytoprotective gene we previously showed to be upregulated by 2MeSADP, also controlled the activity of PTP. Taken together, ATP, acting on $P2Y_1$ receptors, upregulates the PTP expression and its activity, which counteracts the H_2O_2-promoted death signaling cascades including ERK1/2 and its upstream signal src tyrosine kinase in astrocytes.

INTRODUCTION

Adenosine 5′-triphosphate (ATP) is an important signaling molecule that mediates gliotransmission and also glia-to-neuron communication in the CNS (Fields and Stevens-Graham, 2002; Hansson and Ronnback, 2003; Inoue, 2002). The $P2Y_1$ receptor has a central role in the ATP-mediated gliotransmission in astrocytes (Fam et al., 2000) and we previously demonstrated that ATP, acting on $P2Y_1$ receptors, protected astrocytes against oxidative stress, indicating the physiological importance of ATP-mediated gliotransmission in astrocytes (Shinozaki et al., 2005). However, details concerning the molecular mechanism(s) by which $P2Y_1$ receptor activation results in such protection are still lacking.

Hydrogen peroxide (H_2O_2), one of the reactive oxygen species (ROS), activates various intracellular signaling cascades including mitogen-activated protein kinases (MAPKs) (Fialkow et al., 1994; Konishi et al., 1999; Ushio-Fukai et al., 1999). The MAPK family includes extracellular signal-regulated kinase 1 and 2 (ERK1/2), p38 kinase, and c-Jun NH_2-terminal kinase (JNK). The latter two members are well known to be stress-responding MAPKs, which are activated by lipopolysaccharide, cytokines, and oxidative stress such as by H_2O_2 and induce cell death (Oppenheim, 1991). ERK1/2 is constitutively expressed in various regions including the CNS (Boulton et al., 1991). ERK1/2 is activated by various neurotransmitters, hormones and growth factors in physiological conditions, controls the transcription factor activity and induces various physiological responses, such as cell proliferation or differentiation (Boulton et al., 1991; Marshall, 1995; Segal and Greenberg, 1996). However, ERK1/2 is also activated by various types of stress such as oxidative stress or shear stress, and appears to control the survival of cells (Guyton et al., 1996; Takahashi and Berk, 1996; Wang et al., 1998; Xia et al., 1995). Concerning neuronal cells, recent reports have shown that activation of ERK1/2 even promotes cell death both in vivo and in vitro (Murray et al., 1998; Namura et al., 2001; Stanciu and DeFranco, 2002; Subramaniam et al., 2004). Thus, although ERK1/2 is an essential intracellular signaling molecule that mediates various physiological functions, it may also mediate the death of cells. The intensity of ERK1/2 activation and spatial and temporal differences in its activation would greatly affect physiological or pathophysiological events in cells.

The src family, a well-known protein tyrosine kinase (PTK), regulates a variety of cellular functions such as cell

Grant sponsor: The National Institute of Biomedical Innovation, MF-16 grant; Grant sponsor: Uehara Memorial Foundation; Grant sponsor: Scientific Research (B) for Young Scientists (A) and on Priority Areas (A), Ministry of Education, Science, Sports and Culture, Japan.

*Correspondence to: Kazuhide Inoue, Department of Molecular and System Pharmacology, Graduate School of Pharmaceutical Sciences, Kyushu University, Maidashi 3-1-1, Higashi-ku, Fukuoka 812-8582, Japan.
E-mail: inoue@phar.kyushu-u.ac.jp

Received 1 December 2005; Revised 21 July 2006; Accepted 25 July 2006

DOI 10.1002/glia.20408

Published online 30 August 2006 in Wiley InterScience (www.interscience.wiley.com).

growth, proliferation, and differentiation. The src family is abundantly expressed in the CNS (Brugge et al., 1985; Sugrue et al., 1990), and is also involved in brain injury induced by oxidative stress. In fact, H_2O_2 or ischemia/reperfusion injury activates the src family in the hippocampus (Guo et al., 2003; Ohtsuki et al., 1996). Activation of the src family is prevented by protein tyrosine phosphatase (PTP). PTP is related to various events in the CNS such as inhibition of the NMDA receptor activation in neurons(Yu and Salter, 1999) and of microglial TNFa and nitric oxide generation by amyloid β (Tan et al., 2000). In addition, PTP upregulation is observed in kainic acid-treated (Boschert et al., 1997) and ischemia-injured neurons (Takano et al., 1996). Thus, the activity and expression of PTP is also important for the regulation of pathophysiological cellular functions as well as the regulation of src tyrosine kinase.

On the basis of these findings, we hypothesized that MAPKs and src family are key molecules for promoting the H_2O_2-evoked cell death in astrocytes and that ATP acting on $P2Y_1$ receptors may counteract these cell death-promoting signaling cascades.

In the present study, we demonstrate that activation of both src tyrosine kinase and the subsequent ERK1/2 are key events in the H_2O_2-evoked cell death in astrocytes. We also demonstrate that ATP/$P2Y_1$ receptor activation interferes with the H_2O_2-evoked src family—ERK1/2 cascades by increasing the expression and activity of PTP, thereby leading to protection against H_2O_2-induced cell death in astrocytes.

MATERIALS AND METHODS

Chemicals

Adenosine 5′-triphosphate (ATP), adenosine, 2-methylthio adenosine diphosphate (2MeSADP), bovine serum albumin (BSA), propidium iodide (PI), sodium orthovanadate (Na_3VO_4), MRS2179, and *N*-acetyl cystein were purchased from Sigma Chemical (St Louis, MO). The sources of other chemicals are shown in parentheses as follows; hydrogen peroxide (H_2O_2) (Wako Pure Chemicals, Osaka, Japan), 3-(4,5-dimethylthiazol-2-yl)-2,5-diphenyltetrazolium bromide (MTT) assay kit (CHEMICON International, Temecula, CA), PD98059, U0126, SB203580, SP600125, and PP3 (Calbiochem Biosciences, San Diego), PP1 and PP2 (Biosource, CA), auranofin (Alexis biochemicals, Lausen, Switzerland).

Abbreviations

ATP	adenosine 5′-triphosphate
2MeSADP	2-methylthio-adenosine 5′-diphosphate
ERK1/2	extracellular signal-regulated kinase 1 and 2
H_2O_2	hydrogen peroxide
JNK	c-Jun NH_2-terminal kinase
MAPK	mitogen-activated protein kinase
MAPKP	MAPK phosphatase
MEK1/2	MAPK kinase 1 and 2
Na_3VO_4	sodium orthovanadate
PI	propidium iodide
PTK	protein tyrosine kinase
PTP	protein tyrosine phosphatase
P-Tyr	phosphorylated tyrosine
ROS	reactive oxygen species
TrxR	thioredoxin reductase

Antibodies

Polyclonal antibodies against total ERK1/2, phosphorylated ERK1/2, phosphorylated p38, and phosphorylated JNK were purchased from Cell Signaling Technology (Beverly, MA). The monoclonal antibody against phosphorylated tyrosine was purchased from Sigma Chemical (St Louis, MO).

Cells and Cell Culture

Astrocytes were prepared from neonatal rat forebrain. The cells were cultured as previously reported (Shinozaki et al., 2005). For the cell viability assay, cells were seeded on 96-well plates (NUNC, Roskilde, Denmark) at a density of 1.25×10^4 cells/well.

Cell Viability Assay

For the cell viability assay, we used an MTT assay as previously reported (Shinozaki et al., 2005). A 1/10 volume of MTT solution (5 mg/mL in PBS) was added and incubated for 4 h under 10% CO_2/90% air at 37°C. Then, an equal volume of isopropanol (with 0.04 N HCl) was added to the cells. The absorbance was measured on an ELISA plate reader (ASYS Hitech, Eugendorf, Austria) with a test and reference wavelength of 570 and 630 nm, respectively.

Western Blotting

Astrocytes were prepared as described above. After H_2O_2-stimulation, cells were lysed and the lysates were resolved with 10% SDS-PAGE gels and transferred to PVDF membranes. The membranes were blocked for 1 h in Tris-buffered saline containing 0.1% Tween-20 (TBS/T) and 5% non-fat dry milk at room temperature. Then the membranes were incubated with primary antibody dilution buffer (1:1000 dilution into TBS/T containing 5% BSA) overnight at 4°C. After three washes with TBS/T, the membranes were incubated with horseradish peroxidase-conjugated anti-rabbit antibody (1:2000 dilution into TBS/T containing 5% non-fat dry milk) for 1 h at room temperature. The membranes were washed with TBS/T three times, and the proteins were visualized by chemiluminescence. The antibodies for anti-phospho-proteins used in the present study (anti-P-ERK1/2, P-p38, and P-JNK or P-Tyr antibodies) specifically detected only the activated and phosphorylated form of the proteins. To detect total ERK1/2, the aliquot of the same sample was resolved with 10% SDS-PAGE gels, transferred to PVDF membranes in the same conditions and exposed to anti-total ERK1/2 antibody.

Quantification of the Intensity of P-ERK1/2 Bands

To quantify the intensity of P-ERK1/2 bands, we used Image J (http://rsb.info.nih.gov/ij/). P-ERK1/2 bands were selected by rectangular selection. Then, we selected *Analyze-Gels-Select First Lane* from the menu bar. The

area corresponding to each band was measured using *Wand (tracing) tool* from the tool bar.

Immunocytochemistry

After each treatment, the cells were fixed for 30 min at room temperature in 3.7% paraformaldehyde. The fixed cells were permeabilized with PBS containing 0.1% Triton X-100 for 5 min at room temperature and then incubated with the polyclonal anti-ERK1/2 and anti-phospho-ERK1/2 antibodies for 24 h at 4°C. After washing, the cells were incubated with the appropriate secondary antibodies conjugated to Alexa 488 or 546, washed again, and mounted on glass coverslips (Matsunami Glass, Osaka, Japan). Astrocytes for immunocytochemistry were selected randomly. Images were collected in an MRC-1024 laser-scanning microscope (Bio-Rad) with 20× objective lenses. For the comparison of double-stained patterns, images were processed using Photoshop 5 (Adobe System, Mountain View, CA).

Tyrosine Phosphatase Assay

The tyrosine phosphatase activity was measured using a universal tyrosine phosphatase kit (Takara, Shiga, Japan). The measurement was done according to the manufacturer's instructions. Cells were lysed by lysis buffer and transferred into 96-well ELISA plates at a volume of 50 μL/well followed by incubation for 45 min at 37°C. After four times washing with tween-PBS (PBS containing 0.05% tween20), blocking buffer was added to the wells at a volume of 100 μL/well followed by 30 min incubation at 37°C. Then, the blocking buffer was discarded and coloring substrates were added to the wells (100 μL/well). After a 15 min incubation at room temperature, 1 N sulfuric acid was added to the wells (100 μL/well) to stop the reaction. The absorbance was measured by a plate reader (ASYS Hitech, Eugendorf, Austria) at a test wavelength of 450 nm.

Quantitative RT-PCR of PTP Genes

RT-PCR amplifications were performed using Taqman One-step RT-PCR Master Mix Reagents and 200 nM PTP specific primers as previously reported (Shinozaki et al., 2005). Using the computer software Primer Express (Applied Biosystems), clone-specific primers were designed to recognized rat PTP genes, i.e., rat PTP4a1 (Taqman probe, 5′-acacaatccaaccaatgcgaccttaaa-caa-3′; forward, 5′-tgctcctgtggaagtcacataca-3′; reverse, 5′-gtcgtaagttgcttcgcatactctta-3′) and rat PTPro (Taqman probe, 5′-ccgctatacaaacatcctgccgtacgactt-3′; forward, 5′-ttccgctgaaccgatgtaaaa-3′; reverse, 5′-tgaggtgagttgtagc-caggaata-3′). RT-PCR was performed by 30 min reverse transcription at 48°C, 10 min Amplitaq Gold activation at 95°C, then 15-s denaturation at 95°C, 1 min annealing and elongation at 60°C for 40 cycle in a PRISM7700 (Applied Biosystems). Each experiment was performed in triplicate.

RESULTS

MEK1/2 Inhibitors Protect Astrocytes Against H_2O_2-Evoked Cell Death

Figure 1A shows the effect of H_2O_2 on the activation of MAPKs in astrocytes. Western blotting analysis revealed that stimulation of astrocytes with 250 μM H_2O_2 for 2 h resulted in the activation of three MAPKs, i.e., ERK1/2, p38, and JNK (Fig. 1A). We then tested pharmacologically whether the activation of these MAPKs is involved in the H_2O_2-evoked cell death in astrocytes. The H_2O_2-induced decrease in the cell viability of the astrocytes obtained from the MTT assay was always accompanied by the activation of caspase-3, DNA damage, and nucleus condensation (data not shown). Thus, we defined the decrease in cell viability as cell death in astrocytes in the following experiments. MAPK kinase 1/2 (MEK1/2) activates ERK1/2. The MEK1/2 inhibitors PD98059 (10 μM) (Alessi et al., 1995) and U0126 (20 μM) (Favata et al., 1998) strongly inhibited the H_2O_2-evoked cell death (Fig. 1B). The inhibitory

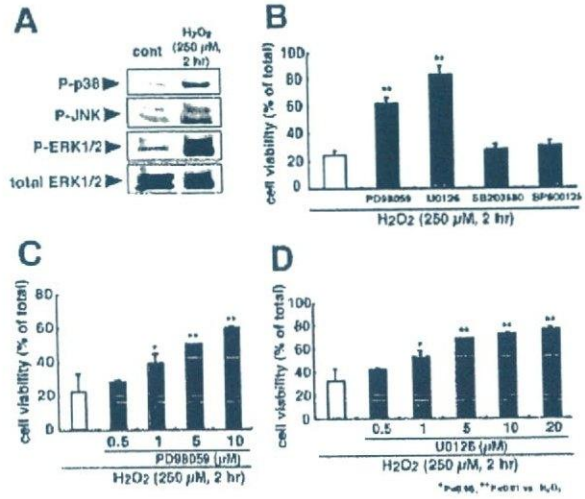

Fig. 1. The effect of MAPK inhibitors on the H_2O_2-evoked cell death of astrocytes. A: The effect of H_2O_2 on MAPK activation in astrocytes. H_2O_2 (250 μM, 2 h) activated p38, JNK, and ERK1/2. B: The effect of MAPK inhibitors on H_2O_2-evoked cell death. The MEK1/2 inhibitors PD98059 (10 μM) and U0126 (20 μM) strongly inhibited the H_2O_2-evoked cell death. Neither the JNK inhibitor SP600125 (20 μM) nor the p38 inhibitor SB203580 (20 μM) affected the H_2O_2-evoked cell death. C: The concentration-dependent effect of PD98059 against H_2O_2-evoked cell death. The protective effect of PD98059 was dose-dependent in a concentration range from 0.5 to 10 μM. D: The concentration-dependent effect of U0126 against H_2O_2-evoked cell death. The protective effect of U0126 was dose-dependent in a concentration range from 0.5 to 20 μM. Neither inhibitor alone affected the cell viability of the astrocytes. Inhibitors added to the cells 1 h before H_2O_2 treatment. Asterisks show significant difference from the response evoked by H_2O_2 ($^*P < 0.05$, $^{**}P < 0.01$ vs. H_2O_2 alone, Student's *t*-test). Results were expressed as means ± SEM of triplicate measurements ($n = 3$).

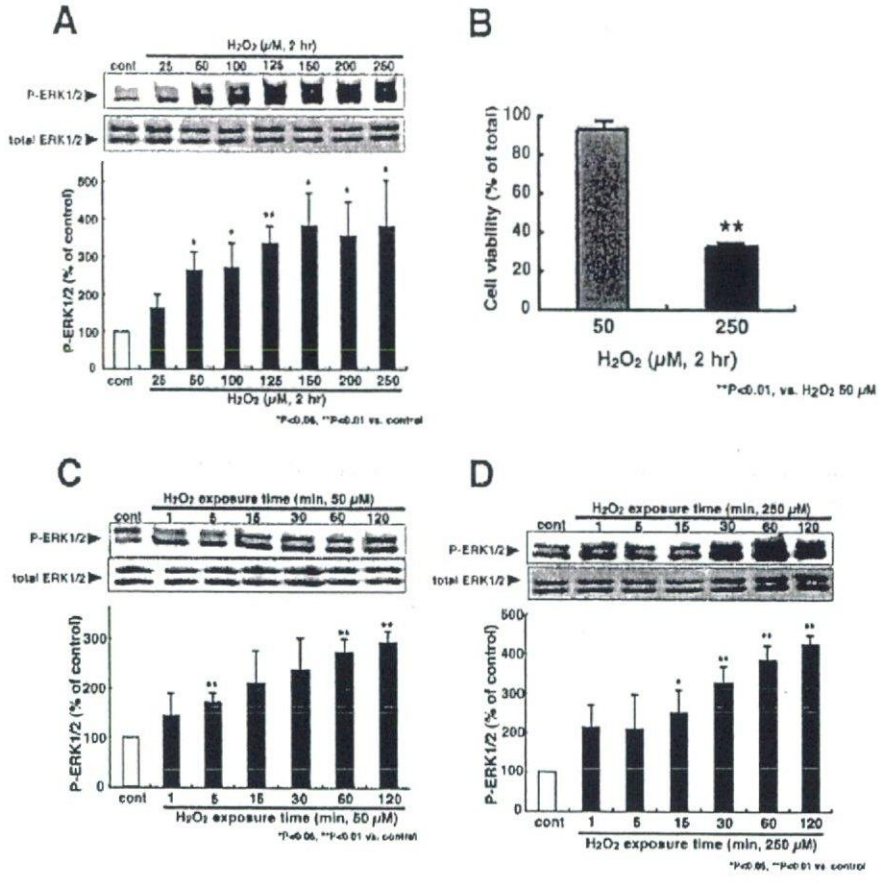

Fig. 2. The concentration-dependency and time course of the H_2O_2-evoked ERK1/2 activation in the astrocytes. **A**: The concentration-dependency of the H_2O_2-evoked ERK1/2 activation. H_2O_2 activated ERK1/2 in a concentration-dependent fashion at the whole cell level (0–250 μM, 2 h). H_2O_2 did not affect the amount of total ERK1/2. Asterisks show significant difference from control ($^*P < 0.05$, $^{**}P < 0.01$ vs. control, Student's *t*-test). **B**: The degree of the decrease of the cell viability of H_2O_2-treated astrocytes markedly decreased the cell viability in the astrocytes 250 μM but not at 50 μM H_2O_2. Asterisks show significant difference from the response evoked by H_2O_2 ($^{**}P < 0.01$ vs. 50 μM H_2O_2, Student's *t*-test). **C** and **D**: A temporal analysis of the H_2O_2-evoked ERK1/2 activation in the astrocytes. At the whole cell level, ERK1/2 was activated by H_2O_2 treatment time dependently (0–120 min) despite the concentration of H_2O_2 (50 and 250 μM). H_2O_2 did not affect the total ERK1/2. Asterisks show significant difference from control ($^*P < 0.05$, $^{**}P < 0.01$ vs. control, Student's *t*-test). Results were expressed as means ± SEM of triplicate measurements ($n = 3$).

effects by PD98059 and U0126 were dose-dependent in a concentration-range from 0.5 to 10 μM (Fig. 1C) and 0.5 to 20 μM (Fig. 1D), respectively. In contrast, neither the p38 inhibitor SB203580 (Alessandrini et al., 1999; McLaughlin et al., 1996) nor the JNK inhibitor SP600125 (20 μM) (Bennett et al., 2001) had any effect on the H_2O_2-evoked cell death.

The Concentration-Dependency and Time Course of H_2O_2-Evoked ERK1/2 Activation

Among the H_2O_2-activated MAPKs tested, only ERK1/2 was involved in the H_2O_2-evoked cell death (Fig. 1B). H_2O_2 activated ERK1/2 in a concentration- and exposure time-dependent fashion at the whole cell level (Figs. 2A,C,D). Although a lower H_2O_2 concentration (50 μM) activated ERK1/2, H_2O_2 at this concentration did not cause cell death (Fig. 2B). At a higher concentration, H_2O_2 (250 μM) evoked ERK1/2 phosphorylation and cell death in astrocytes (Figs. 2A,B). The phosphorylation of ERK1/2 evoked by 250 μM H_2O_2 was stronger than that evoked by 50 μM H_2O_2. H_2O_2 at either concentration did not affect the total ERK1/2 at the whole cell level.

The Temporal and Spatial Aspect of P-ERK1/2 Induced by H_2O_2

We investigated the temporal and spatial distribution of P-ERK1/2 using immunocytochemical techniques. H_2O_2-evoked ERK1/2 activation was observed in GFAP-positive astrocytes (data not shown). It was reported that ERK1/2 is translocated into the nucleus from the cytoplasm when it is activated (Chen et al., 1992; Gonzalez et al., 1993). We thus analyzed the distribution of P-ERK1/2 after H_2O_2 stimulation. When the cells were stimulated with 250 μM H_2O_2 for 2 h, P-ERK1/2 signals were observed in the center part of individual astrocytes and were colocalized with the signals of PI, a DNA binding dye, suggesting that P-ERK1/2 had translocated into the nucleus (Fig. 3A). In contrast, when stimulated with 50 μM H_2O_2 for 2 h which activated ERK1/2 but did not induce cell death, the P-ERK1/2 signals were observed but were not colocalized with the PI signals (Fig. 3A). The total amount of ERK1/2 signals, however, was not affected by H_2O_2 (50 and 250 μM), and they were not colocalized with the PI signals (Fig. 3B). Without H_2O_2 stimulation, the P-ERK1/2 signals were too low (Figs. 2A,D and 3E, cont.) to detect. To quantify the degree of the colocalization of the P-ERK1/2 and PI signals, we

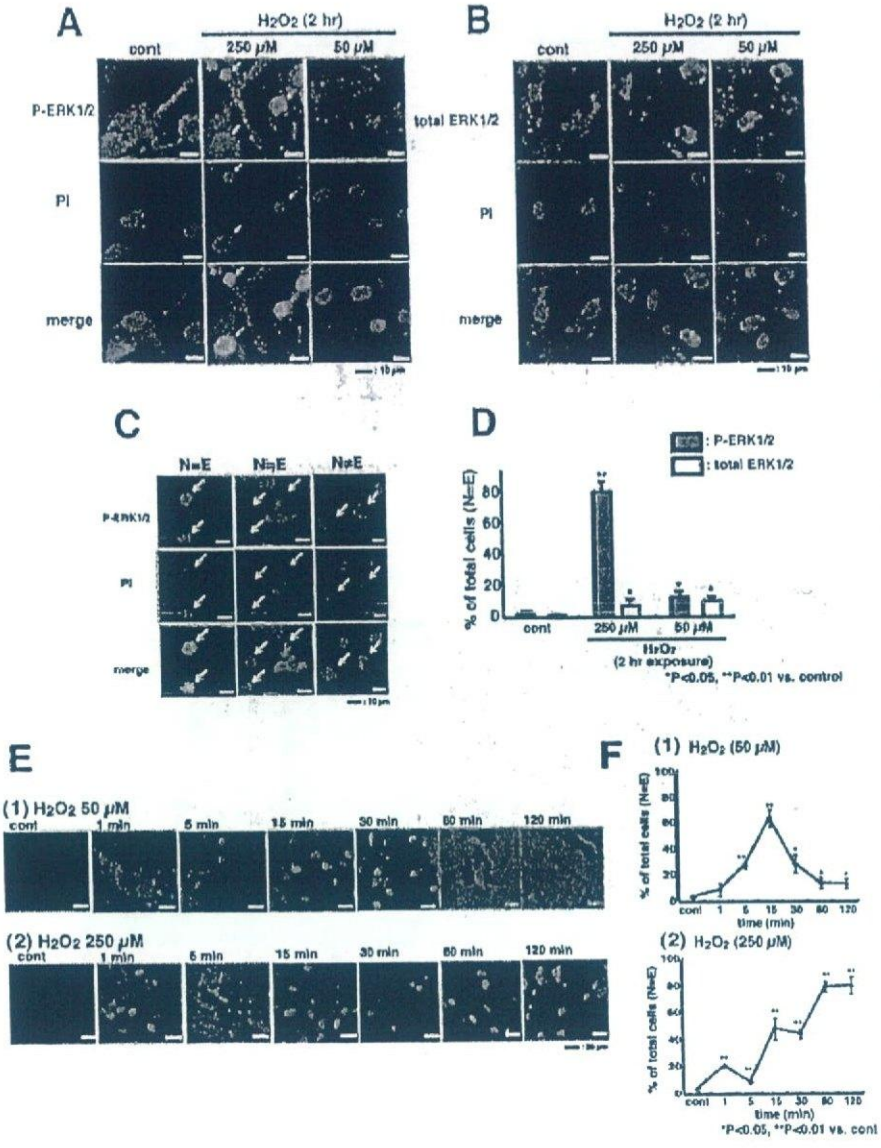

Fig. 3. The effect of H_2O_2 on the intracellular localization of ERK1/2 in astrocytes. A: The effect of H_2O_2 on the intracellular localization of P-ERK1/2. In control, the P-ERK1/2 and PI signals did not colocalize (left). When the cells were treated with 250 μM H_2O_2 (2 h), a large number of P-ERK1/2 and PI signals colocalized (center, arrow). At 50 μM H_2O_2, the P-ERK1/2 and PI signals did not colocalize (right). **B**: The effect of H_2O_2 on the intracellular localization of total ERK1/2. Total ERK1/2 did not colocalize with the PI signals irrespective of the H_2O_2 treatment (control, 50 and 250 μM). The signals of P-ERK1/2 were enhanced by photoshop to clarify their intracellular localization. **C**: Classification of the H_2O_2-treated cells into three groups. Astrocytes in which P-ERK1/2 signals were colocalized with PI signals were defined as "N = E" (left), those in which P-ERK1/2 signals were partly colocalized with PI signals were defined as "N ≒ E" (center), and those in which the P-ERK1/2 signals were not colocalized with the PI signals were defined as "N ≠ E" (right). **D**: Quantification of P-ERK1/2 localization into the nucleus. When cells were stimulated by 250 μM H_2O_2, the colocalization of P-ERK1/2 and PI was observed in most cells but not when they were stimulated by 50 μM H_2O_2. Asterisks show significant difference from control ($^*P < 0.05$, $^{**}P < 0.01$ vs. control, Student's *t*-test). **E** and **F**: The temporal analysis of the colocalization of the P-ERK1/2 and PI signals. At 50 μM H_2O_2, N = E cells increased transiently (5–30 min after H_2O_2 stimulation) (E(1), F(1)). At 250 μM H_2O_2, N = E cells increased time-dependently (E(2), F(2)). The DNA binding dye PI was used for identifying the nuclear region. Asterisks show significant difference from control ($^*P < 0.05$, $^{**}P < 0.01$ vs. control, Student's *t*-test). Results were expressed as means ± SEM of triplicate mensurements.

classified the cells into three groups, i.e., cells in which P-ERK1/2 signals were colocalized with PI signals (defined as "N = E"), those in which the P-ERK1/2 signals were not colocalized with the PI signals (defined as "N ≠ E"), and P-ERK1/2 signals were partly colocalized with IP signals (defined as "N ≒ E") (Fig. 3C). When stimulated with 50 and 250 μM H_2O_2 for 2 h, the fraction of N = E was 12.7% ± 3.8% (n = 304) and 81.0% ± 6.3% (n = 612), respectively. Without H_2O_2 stimulation, no colocalization of P-ERK1/2 and PI was observed in almost any of the cells (N = E cells, 3% ± 0.2%, n = 346) (Fig. 3D). In contrast to P-ERK1/2, most of the total ERK1/2 signals did not colocalize with PI irrespective of H_2O_2 stimulation(N = E cells, control, 1.3% ± 0.8%, n = 225; 250 μM H_2O_2, 6.5% ± 4.0%, n = 545; 50 μM H_2O_2, 10.7% ± 1.2%, n = 229). Furthermore, we analyzed the time course of the fraction of "N = E" cells after H_2O_2 stimulation. When stimulated with 50 μM H_2O_2, the N = E fraction peaked at 15 min after the stimulation, and the fraction decreased to the prestimulated level after 120 min (N = E cells, 1 min, 7.8% ± 5.4%, n = 201; 5 min, 27.8% ± 2.9%, n = 213; 15 min, 66.6% ± 7.1%, n = 216; 30 min, 29.1% ± 7.4%, n = 226; 60 min, 13.1% ± 4.5%, n = 254; 120 min, 12.7% ± 3.8%, n = 405). In contrast, when stimulated with 250 μM H_2O_2, the N = E fraction gradually increased, reached the maximal level at 60 min, and remained even 120 min after the stimulation (N = E cells, 1 min, 20.7% ± 7%, n = 354; 5 min, 8.1% ± 0.7%, n = 213; 15 min, 48.4% ± 8.3%, n = 220; 30 min, 44.2% ± 3.3%, n = 214; 60 min,

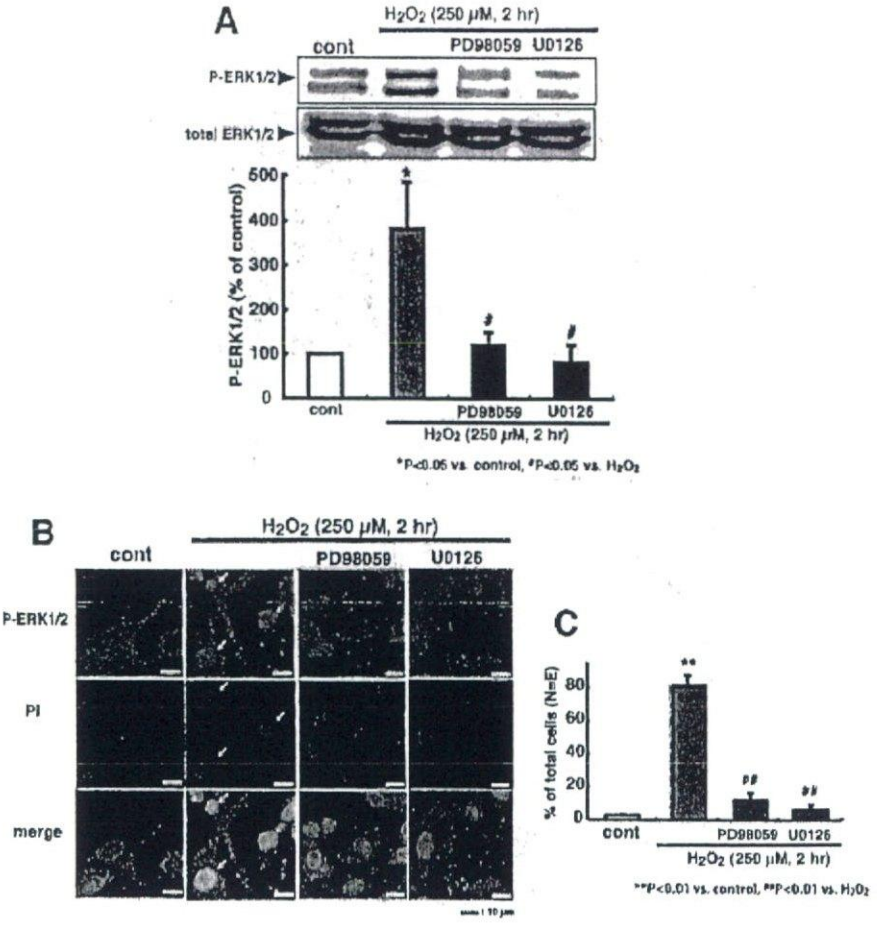

Fig. 4. The effect of MEK1/2 inhibitors on H_2O_2-evoked ERK1/2 activation and P-ERK1/2 translocation. A: The effect of MEK1/2 inhibitors on H_2O_2-evoked ERK1/2 activation. PD98059 (10 μM) and U0126 (20 μM) strongly inhibited the H_2O_2-evoked ERK1/2 activation. Asterisks show significant difference from control ($^*P < 0.05$ vs. control, Student's *t*-test). Sharps show significant difference from H_2O_2 ($^\#P < 0.05$ vs. H_2O_2, Student's *t*-test). Results were expressed as means ± SEM of triplicate measurements ($n = 3$). B and C: The effect of the MEK1/2 inhibitors on the H_2O_2-evoked P-ERK1/2 translocation. PD98059 (10 μM) and U0126 (20 μM) blocked the colocalization of the P-ERK1/2 and PI signals evoked by H_2O_2 (250 μM, 2 h). In the immunocytochemical analysis, the signals of P-ERK1/2 were enhanced by photoshop to clarify their intracellular localization. The DNA binding dye PI was used for identifying the nuclear region. The MEK1/2 inhibitors were applied to the cells 1 h before and during H_2O_2 treatment. Asterisks show significant difference from control ($^{**}P < 0.01$ vs. control, Student's *t*-test). Sharps show significant difference from H_2O_2 ($^{\#\#}P < 0.01$ vs. H_2O_2, Student's *t*-test). Results were expressed as means ± SEM of triplicate measurements.

80.2% ±3.8%, $n = 205$; 120 min, 81%S ± 6.3%, $n = 612$) (Fig. 3F). PD98059 (10 μM) and U0126 (20 μM), at the concentrations that the two inhibitors blocked the H_2O_2-induced cell death (Figs. 1C,D), strongly inhibited the H_2O_2 (250 μM, 2 h)-evoked ERK1/2 activation (Fig. 4A). In addition, these inhibitors prevented the colocalization of P-ERK1/2 and PI, i.e., the H_2O_2-evoked increase in the fraction of N = E was almost abolished (Figs. 4B,C) (N = E cells, PD98059 + H_2O_2, 11.7% ± 3.8%, $n = 524$; U0126 + H_2O_2, 5.9% ± 2.9%, $n = 400$).

ATP Inhibits the H_2O_2-Evoked Activation of ERK1/2 and Its Localization of P-ERK1/2 in the Nucleus

Our previous report by Shinozaki et al., demonstrated that ATP and 2MeSADP inhibited the H_2O_2-induced cell death in astrocytes (Shinozaki et al., 2005). Thus, we examined the effect of ATP and 2MeSADP on the H_2O_2-evoked ERK1/2 activation. In astrocytes pretreated with ATP (100 μM) or 2MeSADP (1 μM) for 24 h, the H_2O_2-induced ERK1/2 activation was markedly inhibited (Fig. 5A). We also analyzed the effect of ATP/2MeSADP on the spatiotemporal behavior of P-ERK1/2 in astrocytes. Immunocytochemical studies showed that pretreatment of the cells with ATP/2MeSADP prevented the H_2O_2-evoked colocalization of P-ERK1/2 and PI signals (Fig. 5B). The fraction of N = E was almost completely inhibited by ATP or 2MeSADP (N = E cells, ATP + H_2O_2, 5.1% ± 3.3%, $n = 340$; 2MeSADP + H_2O_2, 1.1% ± 1.4%, $n = 342$) (Fig. 5C).

ATP itself is known to activate ERK1/2 in some cells including astrocytes (Neary et al., 1999, 2003). Using Western blotting analysis, we found that both ATP (100 μM) and 2MeSADP (1 μM) activated ERK1/2 but the activation was only transient (lasting 1–15 min after stimulation) and returned to the prestimulated level within 120 min [Figs. 6A(i,ii)]. Thus, after the initial phosphorylation of ERK1/2 evoked by ATP/2MeSADP the activation should have returned to the prestimulated level when the astrocytes were stimulated with H_2O_2 24 h after ATP-treatment. Interestingly, when 2MeSADP was pretreated with PD98059 (10 μM) or U0126 (20 μM), the 2MeSADP-induced cytoprotective effects against H_2O_2 disappeared (Fig. 6B). Furthermore, using quantitative RT-PCR, we found that U0126 inhibited the 2MeSADP (1 μM, 2 h)-induced upregula-

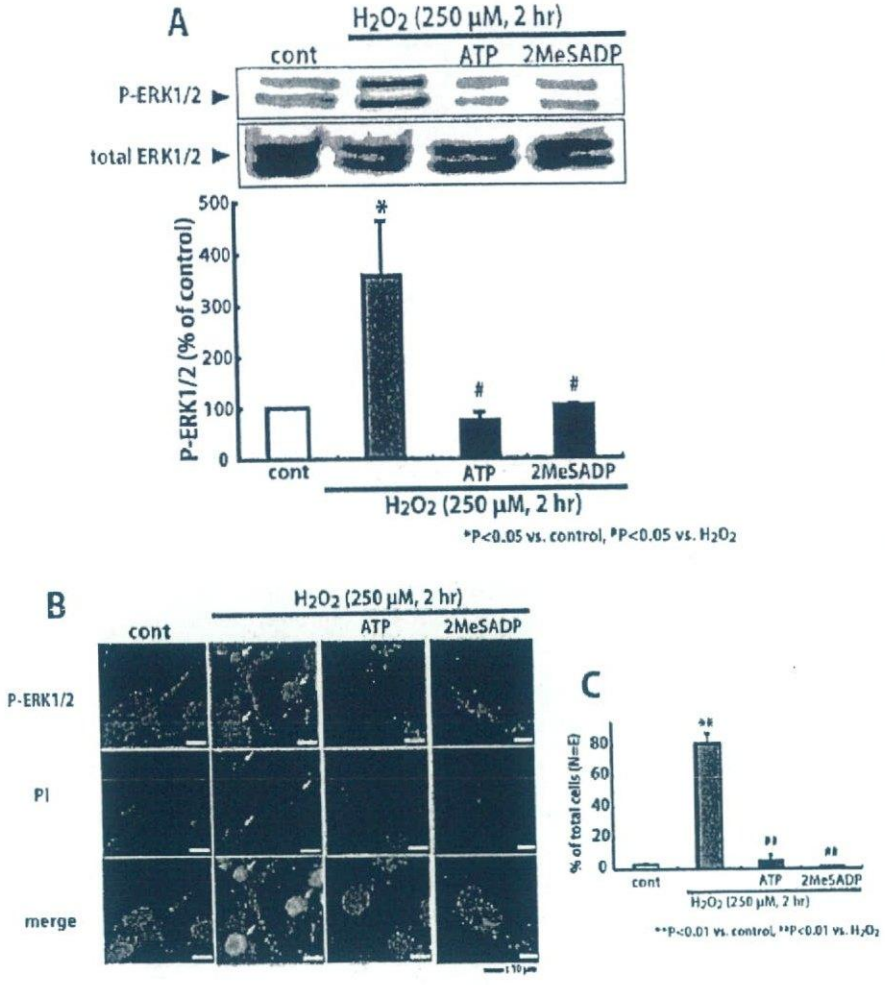

Fig. 5. The effect of ATP and 2MeSADP on H_2O_2-evoked ERK1/2 and P-ERK1/2 translocation. A: The effect of ATP and 2MeSADP on H_2O_2-evoked ERK1/2 activation. ATP (100 μM) and 2MeSADP (1 μM) strongly inhibited the H_2O_2-evoked ERK1/2 activation at the whole cell level. Asterisks show significant difference from control ($^*P < 0.05$ vs. control, Student's *t*-test). Sharps show significant difference from H_2O_2 ($^\#P < 0.05$ vs. H_2O_2, Student's *t*-test). Results were expressed as means ± SEM of triplicate measurements ($n = 3$). B and C: The effect of ATP and 2MeSADP on H_2O_2-evoked P-ERK1/2 translocation. ATP (100 μM) and 2MeSADP (1 μM) abolished the colocalization of the P-ERK1/2 and PI signals evoked by H_2O_2 (250 μM, 2 h). In the immunocytochemical analysis, the signals of P-ERK1/2 were enhanced by photoshop to clarify their intracellular localization. The DNA binding dye PI was used for identifying the nuclear region. ATP and 2MeSADP was applied to the cells 24 h before and during H_2O_2 treatment. Asterisks show significant difference from control ($^{**}P < 0.01$ vs. control, Student's *t*-test). Sharps show significant difference from H_2O_2 ($^{\#\#}P < 0.01$ vs. H_2O_2, Student's *t*-test). Results were expressed as means ± SEM of triplicate measurements.

tion of thioredoxin reductase (TrxR) (2MeSADP, 232.2% ± 54.4% of control, $P < 0.01$ vs. control; 2MeSADP + U0126, 114.9% ± 9.4% of control, $P < 0.05$ vs. 2MeSADP alone; $n = 3$) and PTPs (PTP4a1: 2MeSADP, 291.1% ± 78.5% of control, $P < 0.05$ vs. control, 2MeSADP + U0126, 102.8% ± 12.2% of control, $P < 0.05$ vs. 2MeSADP alone; $n = 3$; PTPro: 2MeSADP, 608.0% ± 153.8% of control, $P < 0.01$ vs. control; 2MeSADP + U0126, 264.7% ± 47.7% of control, $P < 0.05$ vs. 2MeDADP alone; $n = 3$). U0126 alone did not affect the expression level of TrxR (94.5% ± 30.8% of control; $n = 4$) and PTP genes (PTP4a1, 107.5% ± 21.7% of control; PTPro, 113.6% ± 14.3% of control, $n = 4$). The MEK1/2 inhibitors were added to the cells 1 h before and during 2MeSADP-treatment, and was washed out before the H_2O_2 stimulation. Thus, the phosphorylation of ERK1/2 induced by H_2O_2, represented by the sustained and intense responses seen mainly in the nucleus appeared to cause cell death in the astrocytes, while the ATP-induced transient phosphorylation of ERK1/2 appeared to have a cytoprotective action.

ATP Increases PTP Expression and Its Activity, Leading to Protection Against the H_2O_2-Evoked Cell Death in Astrocytes

We comprehensively studied whether ATP induces the expression of genes that could regulate ERK1/2 activity using a GeneChip microarray. We expected that ATP might upregulate the expression of genes that dephosphorylate ERK1/2 such as MAPK phosphatase (MAPKP), which dephosphorylates ERK1/2, thereby leading to the inactivation of ERK1/2 and the cytoprotective action by ATP. However, no upregulation of any MAPKPs in the GeneChip microarray was observed. Instead, we found the ATP (100 μM, 2 h)-induced upregulation of PTP genes containing PTP4a1 and PTP, receptor type O (PTPro) (Table I).

In the PTP activity assay, both ATP (100 μM, 24 h) and 2MeSADP (1 μM, 24 h) significantly increased the PTP activity (ATP, 148.3% ± 8.8%; 2MeSADP, 168.8% ± 4.8%) (Fig. 7A). Subsequently, we analyzed the effect of the PTP inhibitor sodium orthovanadate (Na_3VO_4)